Journal of Hazardous Materials 246–247 (2013) 119–125

Contents lists available at SciVerse ScienceDirect

Journal of Hazardous Materials

journal homepage: www.elsevier.com/locate/jhazmat

Immobilization of horseradish peroxidase by electrospun fibrous membranes for adsorption and degradation of pentachlorophenol in water

Junfeng Niu*, Jiangjie Xu, Yunrong Dai, Jiale Xu, Huiyuan Guo, Kang Sun, Ruilan Liu

State Key Laboratory of Water Environment Simulation, School of Environment, Beijing Normal University, Beijing 100875, PR China

HIGHLIGHTS

- HRP–EFMs were successfully prepared by emulsion electrospinning.
- HRP–EFMs can adsorb and biodegrade pentachlorophenol (PCP).
- The adsorption and degradation process of PCP was obviously influenced by pH.
- Humic acid decreased the adsorption capacity of PCP on EFMs.
- HRP immobilized on membranes shows better stability than free HRP.

ARTICLE INFO

Article history:
Received 5 July 2012
Received in revised form
10 December 2012
Accepted 11 December 2012
Available online 20 December 2012

Keywords:
Electrospun fibrous membrane
Immobilization
Sorption
Biodegradation
Horseradish peroxidase
Pentachlorophenol

ABSTRACT

Horseradish peroxidase (HRP) is successfully *in situ* encapsulated into the poly(D,L-lactide-co-glycolide) (PLGA)/PEO–PPO–PEO (F108) electrospun fibrous membranes (EFMs) by emulsion electrospinning. The adsorption and degradation of pentachlorophenol (PCP) by HRP–EFMs are investigated. The experimental results show that the sorption kinetic of PCP on EFMs follows the pseudo-second-order model, and the sorption capacity is as high as 44.69 mg g^{-1}. The sorption mechanisms of EFMs for PCP can be explained by hydrogen bonding interactions, hydrophobic interactions and π–π bonding interactions. Profiting from the strong adsorption, the removal of PCP can be dramatically enhanced by the interaction of adsorbed PCP and HRP on the surface of EFMs. For PCP degradation, the optimal pH values for free HRP and immobilized HRP are 4 and 2–4, respectively. As pH > 4.7, no adsorption and degradation are observed due to the deprotonation of PCP. The removal percentages reach 83% and 47% for immobilized HRP and free HRP, respectively, at 25 ± 1 °C. The presence of humic acid can inhibit the activity of HRP and decreases the adsorption capacity of PCP because of competitive adsorption. The operational and storage stability of immobilized HRP are highly improved through emulsion electrospinning.

1. Introduction

Pentachlorophenol (PCP) has been widely used as pesticide, wood preservative and herbicide in many agricultural and industrial applications for many years [1,2]. This widely usage of PCP has resulted in the serious pollution of soil and aquatic environments. For example, PCP has been detected out in soil at a relative high concentration of 0.1–4500 mg kg^{-1} in some regions of Sweden [3]. Furthermore, PCP is of bioaccumulation and can concentrate in human liver, kidney and fat *via* food chain. The high concentration of PCP in environment has caused the high detection rate in human body. The related researches conducting in Germany show that the concentration of PCP in human blood reaches as high as 3.14 μg L^{-1} [4]. Unfortunately, PCP is a kind of environmental pollutant with carcinogenicity, teratogenicity and toxicity. It can increase the rate of tumor, and impede reproduction [5]. PCP is listed as priority pollutant by the U.S Environmental Protection Agency.

Many methods including adsorption [6], catalytic oxidation [7] and biodegradation [8] are developed to remove PCP from water. For adsorption, nanomaterials and activated carbon are frequently used as adsorbent [9,10]. It has been found that the rate of adsorption is mainly related to the diffusion of PCP from the aqueous phase to the adsorbent [11,12]. Usually, adsorption is used combining with other methods to eliminate PCP from water [13,14].

Biodegradation has been applied extensively to decompose organic pollutants for its cost-efficient and little secondary pollution. The enzymatic catalysis, an important biodegradation method, is usually used for the removal of organic pollutants from water. It is proven that PCP can be degraded efficiently by the catalysis of horseradish peroxidase (HRP) with the presence of hydrogen peroxide. The intermediate products of the reaction are some kinds of dimers like tetrachloro-*p*-benzoquinone and 2,3,4,5,6-pentachloro-4-pentachlorophenoxy-2,5-cyclohexadienone (PPCHD). They are insoluble and inertia in

* Corresponding author. Tel.: +86 10 5880 7612; fax: +86 10 5880 7612.
E-mail address: junfengn@bnu.edu.cn (J. Niu).

0304-3894/$ – see front matter © 2012 Elsevier B.V. All rights reserved.
http://dx.doi.org/10.1016/j.jhazmat.2012.12.023

aqueous phase but reactive when dissolved in various organic solvents [15–18]. However, the main drawback of treating wastewater by free HRP is its non-renewability and instability. To overcome this shortcoming, immobilization of HRP has been developed as an effective method for the applications of HRP, since it offered many advantages, such as increasing the stability of HRP, and easily being repeated use [19–22]. Among the various immobilization methods just like crosslinking [23], adsorption [24], encapsulation [25], and so on, encapsulation is regarded as a satisfying choice for immobilizing enzyme. It allows enzyme molecules to be fully embedded in the supports and decreases the interaction with the external interface [26,27]. Therefore, it is of great importance to find out an efficient method to encapsulate HRP in the supports.

Emulsion electrospinning, as a simple and economical way to encapsulate enzyme *in situ*, has received more and more attention in decades [28–31]. It is an unique method to produce fibers with a diameter ranging from dozens of nanometers to several micrometers [32]. As the production of emulsion electrospinning, electrospun fibrous membranes (EFMs) have many novel characters, such as porous structure, high surface-to-volume ratio and well mechanical properties. These characters make EFMs adsorbing more pollutant and easier to be recovered [33,34]. Meanwhile, the porous structure of fibers is benefit for the improvement of the mass-transfer rate of substrate to the active site of the enzymes [29]. Thus, EFMs are regarded as a suitable supporter for the immobilization of enzyme. Recently, EFMs have been widely applied in tissue engineering [35], medicine [36], electrochemistry [37], immobilization [38–40], and so on. An extended application of immobilized HRP by emulsion electrospinning for removal of environmental pollutants from contaminated water is desired.

The aim of this study is to immobilize HRP on EFMs by emulsion electrospinning, and use it to remove PCP from water. Herein, poly(D,L-lactide-co-glycolide) (PLGA) is chosen as the polymer for preparation of fibers for its biodegradability, biocompatibility and outstanding mechanical properties. The morphology, structure of EFMs and the enzymatic properties of immobilized HRP are investigated. The adsorption processes of PCP on EFMs and the degradation efficiency of PCP by immobilized HRP are assessed.

2. Materials and methods

2.1. Materials

Poly(D,L-lactide-co-glycolide) (PLGA) (glass transition temperature: 40–55 °C) was prepared by the way of ring opening polymerization. The made-up polymer was purchased from Jinan Daigang biomaterials Co., Ltd. (China). The molecular weight of PLGA was approximately 100,000 g mol^{-1}, and its structural formulas is shown in Fig. S1. Triblock copolymer PEO–PPO–PEO (F108) was purchased from BASF (Germany). Pentachlorophenol was supported by Damao Chemical Reagent Factory (China). Horseradish peroxidase with the 300 U mg^{-1} solid activity was obtained commercially from Nuoqiya Biological Technology Co., Ltd. (China). Methylene dichloride and methanol (HPLC, 99.9%) were provided by J.T. Baker (USA). Hydrogen peroxide (30%) was purchased from Beihua Fine Chemicals Co., Ltd. (China). Fluorescein isothiocynate (FITC) and 2,2-azinobis-3-ethylbenzothiazoline-6-sulfonate (ABTS, 99%) were obtained commercially from Sigma–Aldrich (USA). All other reagents were of analytical grade, without further purification. All solutions were prepared using high-purity water obtained from a Milli-Q Plus/Millipore purification system.

2.2. Preparation of electrospun fibrous membranes

Electrospinning was conducted on a self-made electrospinning apparatus in our laboratory. The procedures for the EFMs were as follows: PLGA (1.8 g) and a certain amount of F108 were dissolved in 15 g methylene dichloride with stirring for 2.0 h at ambient temperature. Then, a volume of 0.3 mL (600 U mL^{-1}) HRP solution was added into the PLGA solution previous and mixed fully to obtain homogeneous emulsions. After that, the emulsion was loaded into a stainless glass syringe equipped with a clean needle (0.5 mm inner diameter), which was connected with a high-voltage power supply (HB-Z503-2AC, China). Electrospinning was operated at a voltage of 10 ± 1 kV, and the emulsion was fed at a rate of 1.5 mL h^{-1} by using a syringe pump (RWD Life Science Company Limited, China). A grounded iron plate, which was covered with aluminum foil, was placed at a distance of 15 cm from the needle tip as a fiber collector. It usually took about 3–5 h to obtain sufficiently thick and integrated EFMs. All experiments were conducted at room temperature (25 ± 1 °C) and a relative humidity of 40 ± 2%.

2.3. Characterization

The morphology of EFMs was observed with a field emission scanning electron microscope (FESEM S-4800, HITACHI, Japan). Two kinds of samples were prepared: one was PLGA/F108–HRP composite fibers electrospun from the emulsion, and the other one was replacing HRP solution with the same amount of pure water. The fiber diameter was calculated from more than 50 counts randomly selected from 10 different SEM images. In order to confirm the presence and distribution of HRP in the fibers, the PLGA/F108-fitc-HRP composite fibers were observed on laser confocal scanning microscopy (LCSM; LSM510, ZEISS, Germany). The excitation and emission wavelengths were 488 and 535 nm, respectively. Specific surface area, pore size and pore volume were obtained by using a full-automatic specific surface area analyzer (Micromeritics ASAP 2020, USA). For the purpose of measuring the contact angle value, the polymer was dissolved in methylene dichloride and then prepared into cast films. The contact angle was tested on a contact angle measuring system (OCA20, Dataphysics, Germany) by high-purity water.

2.4. Activity assays of HRP

The activity of HRP was determined by using ABTS as the substrate. During the experiment, one piece of HRP-EFMs (0.02 ± 0.002 g) was washed three times with high-purity water firstly to elute the HRP on the surface of membranes. Then, the HRP–EFMs was immersed into 5 mL assay mixture consisting of 1.7 mmol L^{-1} ABTS and 0.83 mmol L^{-1} H_2O_2. After 5 min of reaction, an appropriate amount of assay mixture was transferred to a spectrophotometer cuvette. The absorbance change of the solution was measured in a UV–vis spectrophotometer (Cray 50, VARIAN, USA) at a wavelength of 405 nm. The molar extinction coefficient for the oxidation of ABTS at 405 nm is 18 600 M^{-1} cm^{-1}. One unit of activity is defined as the amount of HRP catalyzing the consumption of 1 mmol of peroxide per min.

For assessment of the operational stability, the HRP–EFMs were taken out from the reaction mixture after one assay and transferred to the fresh ABTS solution, and this process was repeated 8 times. The relative activity at each data point was calculated from the ratio of residual activity to initial activity. For testing the storage stability of immobilized HRP, residual activities were measured over the course of 2 months. Before activity measurements, the HRP-EFMs were stored at room temperature (25 ± 5 °C) in a dryer.

2.5. Sorption experiments

Batch experiments were conducted at 25 ± 1 °C in an incubator shaker. Three pieces of EFMs (2 cm × 2 cm, total weight 50 ± 2 mg) were added to 100 mL of PCP aqueous solution, and the reaction

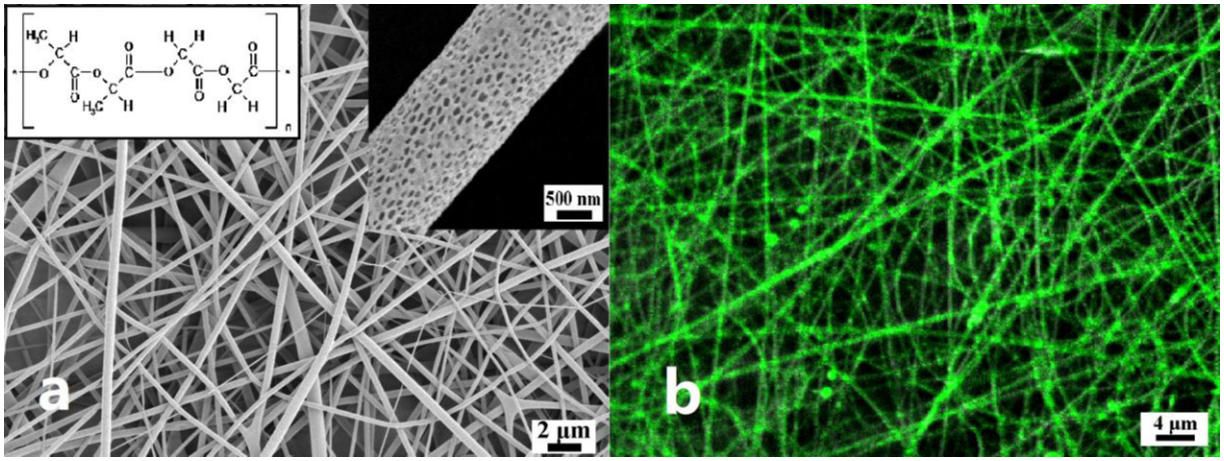

Fig. 1. (a) SEM micrograph of EFMs: the inserted image shows the high resolution image of the pores on the surface of beads; (b) laser confocal microphotograph micrograph of EFMs: the image shows most of fibers emit green fluorescence.

mixture was shaken on a shaker at 160 rounds per minute. In the experiment, sorption kinetic was carried out with an initial PCP concentration of 10 mg L^{-1}. The sorption isotherm experiment was conducted with the pH of 3 and an initial PCP concentration ranging from 1 mg L^{-1} to 13 mg L^{-1}. To avoid cosolvent effect, the methanol volume fraction in each solution was controlled to less than 0.001. According to the preliminary experiment, adsorption equilibrium was reached when the experiment running 120 min. A volume of 1.5 mL reaction sample was taken from the reaction system at certain time intervals for high performance liquid chromatography (HPLC; Waters 2695, USA) analysis. Experimental uncertainties evaluated in samples without EFMs were less than 5% of the initial concentrations. All samples were produced in triplicates including control, and the average value was adopted.

The Langmuir model (LM) and the Freundlich model (FM) were used to fit the isotherm experiment data, and then to compare their goodness of fitting. Moreover, for analyzing the adsorption kinetic data, pseudo-first-order model (PFOM) and pseudo-second-order model (PSOM) were used. The parameter values of all models were calculated by means of the nonlinear curve fitting analysis. The sorption isotherm and kinetics models are listed in Table S1 in Supporting Information.

2.6. Degradation experiments

Three pieces of HRP–EFMs (2 cm × 2 cm, total weight 50 ± 2 mg) were added into 100 mL solutions with the concentration of PCP at 10 mg L^{-1} (or 0.038 mmol L^{-1}) and H_2O_2 at 0.019 mmol L^{-1} due to the molar ratio of the reaction between PCP and H_2O_2 being about 2:1 [1]. The mixtures were incubated with stirring (160 rpm) for 120 min and sampled periodically. For the purpose of terminating HRP catalysis, a volume of 20 μL sodium azide (0.1 mol L^{-1}) was added when sampling. The control experiment for free HRP was carried out in the same reactor using an equivalent amount of HRP. The PCP concentrations in aqueous phase and on/in the HRP–EFMs (washed by acetonitrile) were measured by HPLC as well. The amount of PCP degraded by HRP–EFMs was calculated by the equation:

$$q_D = q_0 - q_S - q_A \quad (2)$$

where q_D is the amount of PCP degraded by HRP–EFMs; q_0 is the initial amount of PCP in solution; q_S is the amount of PCP retained in solution; and q_A is the amount of PCP adsorbed by HRP–EFMs.

The preliminary experiment indicated PCP cannot be degraded by H_2O_2 without the catalysis of HRP. All experiments were carried out at 25 ± 1 °C. All samples were produced in triplicates including control, and the average value was adopted.

3. Results and discussion

3.1. Morphology of electrospun fibrous membranes

As shown in Fig. 1(a), the SEM images of EFMs prepared from the PLGA/F108–water composite solution and EFMs prepared from the PLGA/F108–HRP composite solution exhibited the same characteristics that these fibers possessed the feature of being randomly arrayed and bead-free. The average diameter of the fibers was approximately 600 nm. Some of other properties of EFMs are summarized in Table S2. The results of the pore volume and SEM images prove that plenty of pores exist on the surface of the fibers.

The mechanisms of pores formation during emulsion electrospinning were investigated by some researchers [28,34,41,42]. It is mainly considered as a phase separation mechanism between the polymer and the air phase. Under the influence of strong electric field, the polymers in the solution may be distributed heterogeneously, which result in the formation of polymer-rich and polymer-poor regions on the surface of the fibers. Polymer-poor regions are mainly consisting of volatile methylene dichloride, so the pores are probably formed from the bubbles in polymer-poor regions during the evaporation of the methylene dichloride [34]. The formation of pores is also influenced by the polymer, the solvent and the ambient humidity [42].

The LCSM observations were carried out to verify whether the HRP was encapsulated inside the fibers. The LCSM image presented in Fig. 1(b) illustrates that most of fibers emit green fluorescence, indicating the HRP is immobilized in the fibers successfully and distributes homogeneous.

3.2. The operational and storage stability of immobilized HRP

The operational stability of immobilized HRP was examined by using the same HRP–EFMs for oxidating ABTS repeatedly. As shown in Fig. 2, immobilized HRP retained as high as 60% initial activity after 8 batches of experiments, which is higher than that of macroporous glycidyl methacrylate-based copolymers (45% remained after 4 cycles) [43] and P(DEA-co-AA) microgels (50% remained after 5 cycles) [44], indicating that the operational stability of immobilized HRP is improved. This improvement is mainly attributed to the way enzyme is immobilized and the pore structure of fibers. The HRP was encapsulated in the fibers by emulsion

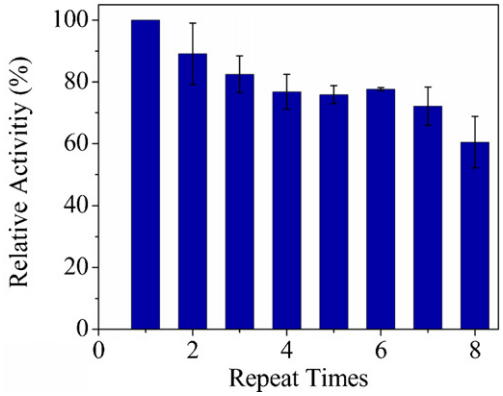

Fig. 2. The operational stability of immobilized HRP (at 25 ± 1 °C, pH 4, with 1.7 mmol L^{-1} ABTS and 0.83 mmol L^{-1} H_2O_2 initially).

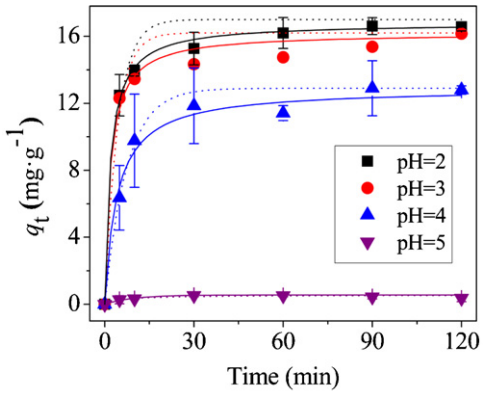

Fig. 3. Sorption kinetics of PCP on ENFMs fitted by pseudo-first-order model (. . .) and pseudo-second-order model (—) (at 25 ± 1 °C with 0.038 mmol L^{-1} PCP initially).

electrospinning, which decreased the interacting with the assay mixture, and keep the activity of HRP during the reaction. At the same time, pores on the fibers can lower the adverse influence of steric hindrance, and increase the access of ABTS to the active site of the HRP.

For assessment of immobilization yield, one piece of HRP–EFMs (0.02 ± 0.002 g) was washed by 3 ml high-purity water. The protein content in water was then measured by using Coomassie brilliant blue staining. The experimental results show that the immobilization yield is about 0.3 mg g^{-1} (90% of the total immobilized HRP), which is higher than that of kaolinite (35.5%), vermiculite (56.2%) and montmorillonite (66.0%) [45]. For assessing recovered activity of the immobilized HRP, the activity of free HRP was detected in the same method described in Section 2.4 by using an equivalent amount of free HRP. The recovered activity of the immobilized HRP was calculated by the equation:

$$R = \frac{A_i}{A_f} \times 100\% \quad (1)$$

where R is the recovered activity of the immobilized HRP; A_i is the activity of immobilized HRP; and A_f is the activity of free HRP. The results indicated that the recovered activity of the immobilized HRP was about 50%. Compared to the recovered activity of HRP immobilized on macroporous glycidyl methacrylate-based copolymers (5.3–42.8%) [43], a relative high recovered activity was obtained. This significant enhancement are mainly attributed to the presence of F108, which exists in the HRP solution (aqueous phase)/methylene dichloride (oil phase) mixed system as a surfactant. During the string process, F108 can wrap HRP solution and form homogeneous emulsions [46,47]. The HRP–F108 structure can protect HRP from the damage of methylene dichloride and decrease the influence of high-voltage electric field when electrospinning, therefore the structure and function of HRP cannot be changed in the immobilizing process. Furthermore, emulsion electrospinning can prepare the core–shell structured fibers. HRP as the water phase of emulsion can be directly encapsulated into the core of electrospun fibers. Under the protection of polymer shell, HRP can get away from the disturbance of external environment and keep high activity for a longer time.

For assessing the storage stability of the immobilized HRP, the activity of HRP–EFMs was estimated for two months. As shown in Fig. S2, it was found that the immobilized HRP could maintain about 50% of its initial activity after two weeks of storage. After two months, the immobilized enzyme still retained over 30% of its initial activity. While free HRP loses its activity in few hours [1]. These results demonstrate that the stability of immobilized HRP is highly improved compared to that of free HRP.

3.3. Sorption properties of EFMs for PCP

3.3.1. Sorption kinetic

Fig. 3 shows the sorption kinetics of PCP on EFMs at different pH values. At pH 2–4, the sorption equilibrium was almost achieved within the first 30 min of the reaction, and then became more gradual until the equilibrium was reached in 120 min. The sorption rates of EFMs for PCP were in direct proportion to the acidity of solution, and its sorption capacities at pH = 2, 3 and 4 were 15.27, 14.33 and 11.85 mg L^{-1} at 30 min, respectively. Meanwhile, almost no adsorption process was observed at pH 5. In order to explain this phenomenon, protonated-deprotonated PCP is introduced. PCP in the solution is predominated by protonated form when the pH is lower than 4.7 (the pK_a for PCP is 4.7), while at higher pH (>4.7) the deprotonated form does [48]. These two PCP forms differ markedly in biological and physical properties. For example, PCP in protonated form shows an obvious hydrophobicity, and it is easier to be adsorbed [49,50]. Thus EFMs show a good adsorptivity for PCP when the solution pH is lower than 4.7.

PFOM and PSOM were applied to describe the sorption kinetics data to further understand the sorption kinetics of PCP on the EFMs. As shown in Table S3, the higher correlation coefficient (r^2) indicates that the PSOM fits the experimental data better than the PFOM. The parameter k_2^* can directly describe adsorption kinetic process as an applicable rate constant. The k_2^* values of PCP on EFMs at pH 2, 3 and 4 were 0.532, 0.529 and 0.293, respectively, which showed a positive relationship between adsorption rate and acidity. It means that the adsorption rate is related to the degree that PCP protonated. This result indicates that the hydrophobicity of PCP exhibits remarkable effect on the sorption rate, indicating that hydrophobic interactions exist during the sorption. Moreover, the good fit of PSOM for kinetics data demonstrate that the chemical interactions may exist in the sorption processes, and it may be π–π bonding interactions introduced by PCP molecules that contain π electrons interacting with the π electrons of the C═O on the polymer surface. Furthermore, the —OH group on PCP can act as hydrogen-bonding donors and form hydrogen bonds with the C═O groups on polymer. Thus, hydrogen bonding interactions, hydrophobic interactions and π–π bonding interaction exist in the sorption processes.

3.3.2. Sorption isotherm

Sorption isotherm is critical to evaluate the sorption capacity of adsorbents and understand the sorbate–sorbent interactions. Two widely used models, the Langmuir and Freundlich equations, were applied to describe the isotherm data. The sorption isotherms for PCP on EFMs are shown in Fig. S3 and Table S4. The results showed that sorption isotherms could be well fitted by both of them,

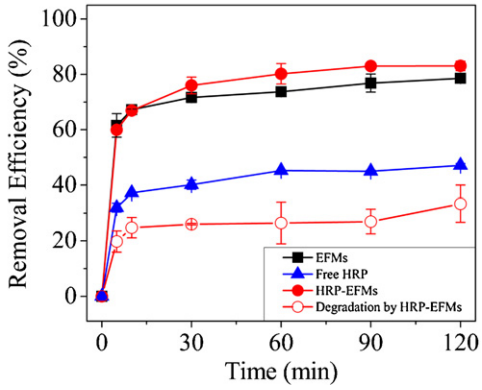

Fig. 4. Degradation kinetic of PCP by free and immobilized HRP (at 25 ± 1 °C and pH 3 with 0.038 mmol L^{-1} PCP and 0.019 mmol L^{-1} H_2O_2 initially).

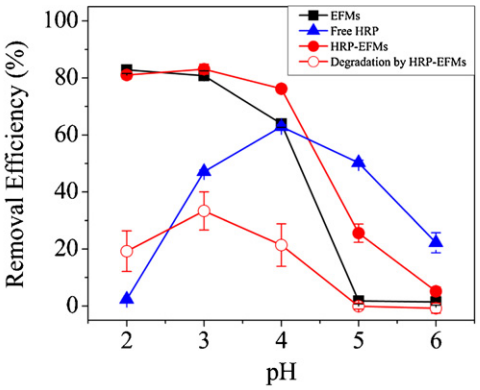

Fig. 5. Effect of pH on the degradation efficiency of PCP by free and immobilized HRP (120 min at 25 ± 1 °C with 0.038 mmol L^{-1} PCP and 0.019 mmol L^{-1} H_2O_2 initially).

supported by the high r^2 values of 0.977 and 0.987, respectively. The relatively higher r^2 value of LM indicates that the sorption of PCP on EFMs may be monolayer sorption. According to the parameter q_m, the sorption capacity is 44.69 mg g^{-1}. The Freundlich model is an empirical isotherm model usually used in heterogeneous surface energy systems. As one of its parameter, n^{-1} is an indicator of nonlinearity. Moreover, $n^{-1} = 1$ means a linear isotherm, and it indicates no sorbate–sorbate interaction exists [51]. According to the results of Freundlich fitting ($n^{-1} = 0.812$), the isotherm is nonlinear. It further demonstrates that hydrophobic, π–π bonding and hydrogen bonding interactions play important roles in the sorption.

3.4. PCP degradation by free and immobilized HRP

3.4.1. Degradation kinetic

Fig. 4 shows the degradation efficiency of PCP in a batch experiment running for 120 min. In the first 30 min, the degradation process of free HRP was fast and reached a degradation percentage of about 40%, and the contribution of free HRP to PCP degradation was about 47% at 120 min. The degradation efficiency of HRP–EFMs is slightly lower than that of free HRP, suggesting that HRP is partly inactivated during electrospinning. However, the removal efficiency of HRP–EFMs is much higher than degradation efficiency. It is due to the fact that the PCP removal by immobilized enzyme is the result of both EFMs adsorption and enzymatic catalysation. Taking EFMs adsorption into consideration, the pure PLGA EFMs are used as control samples.

Comparing the removal efficiency between HRP–EFMs and EFMs, differences were shown after the first 10 min. This phenomenon may be due to the catalysis of HRP. This result shows that the process of PCP adsorbed by EFMs contains two steps: (1) PCP molecules diffuse from the bulk solution to the external surfaces of the EFMs, and adsorb onto those easily accessible hydrophobic sites on the surface [52]; and (2) PCP molecules diffuse into the fibers through pores [53]. In the first step, a great amount of PCP is degraded by the HRP which is immobilized on the surface of fibers, and this step is usually assumed to be a fast one. During the second step, some diffused PCP is degraded by the HRP encapsulated in fibers and this step is relative slow.

3.4.2. Effect of pH

The pH of solution influences the activity of enzyme and determines the form of PCP. Therefore, it is of great importance to understand the effect of pH on the removal of PCP from water. As shown in Fig. 5, the pH of solutions varies from 2 to 6. The optimal pH for free HRP was about 4. A higher degradation efficiency of PCP by HRP–EFMs occurred under a pH range from 2 to 4, and the optimal pH was 3, at which the highest PCP removal (83%) was achieved. The immobilized HRP shows a broadening pH range of enzyme catalysis activity, which makes the immobilized HRP suitable for the removal of more practical industrial effluents. However, nearly no PCP was degraded by HRP–EFMs when pH is 5 and 6. This phenomenon mostly attributes to the pK_a (4.7) of PCP. As pH > 4.7, PCP mainly exists in deprotonated form and is hard to be adsorbed by EFMs, thus immobilized HRP gets less chance to react with PCP.

3.4.3. Effect of temperature

The results of batch experiments conducting at the temperature 45, 35, 25 and 15 °C are shown in Fig. 6. Free HRP and immobilized HRP shared the same optimal temperature at 25 ± 1 °C and removal percentage reached 83% for immobilized HRP and 47% for free HRP. Comparing with 25 °C, the removal efficiency of both HRP–EFMs and EFMs decreased much (about 25%) at 15 °C, indicating the adsorption process of PCP to EFMs was an endothermic reaction.

For temperature 35 °C, the removal efficiency of both HRP–EFMs and EFMs was much lower than that at 25 °C, as a result of the temperature being approach to the glass transition temperature of PLGA (40–55 °C) and the structure of EFMs getting to change. During the experiments, it was observed that EFMs shrink and harden at 45 °C, further demonstrating the structure of EFMs has changed. As shown in Fig. S4, no desorption process happens during the reaction. This phenomenon indicates the change of EFMs structure does not lead to EFMs releasing adsorbed PCP. Although the change of temperature influence the removal efficiency obviously for both free HRP and HRP–ENFMs, immobilized HRP shows a better toleration than free HRP.

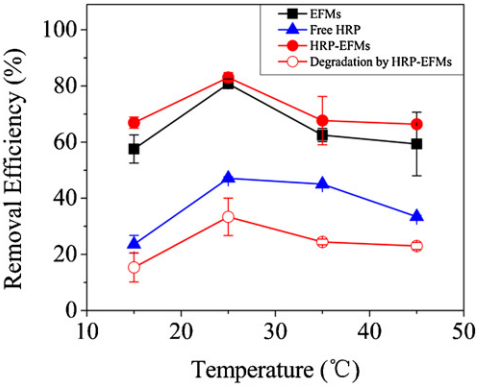

Fig. 6. Effect of temperature on the degradation efficiency of PCP by free and immobilized HRP (120 min at pH 3 with 0.038 mmol L^{-1} PCP and 0.019 mmol L^{-1} H_2O_2 initially).

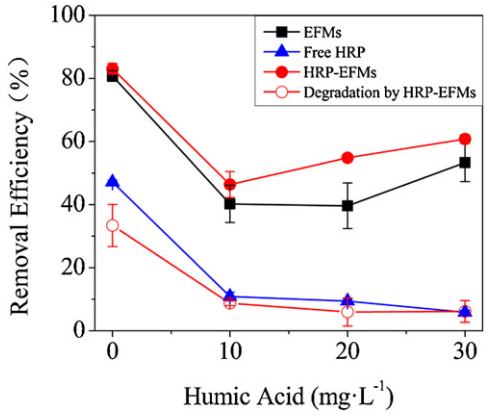

Fig. 7. Effect of humic acid on the degradation efficiency of PCP by free and immobilized HRP (120 min at 25 ± 1 °C, pH 3 with 0.038 mmol L^{-1} PCP and 0.019 mmol L^{-1} H_2O_2 initially).

3.4.4. *Effect of humic acid*

Humic substances arise from microbial degradation of plants and animals. They are ubiquitous in natural water bodies. Some researchers found that humic acid can inhibit the activities of some biomacromolecule [54–56]. Therefore it is important to understand their effect on the removal of PCP from water. In this study, humic acid was used to quantify such an effect. The used humic acid solution was prepared by dissolving humic acid powder in high-purity water. The concentration of humic acid was confirmed by TOC analyzer. The results are shown in Fig. 7. Humic acid shows an obvious inhibitory action to the activity of both free HRP and immobilized HRP, and the inhibitory effect is positive correlation with the concentration of humic acid.

The presence of humic acid decreased the adsorption capacity of PCP. This phenomenon may result from the competitive adsorption, because humic acid molecules are macromolecules, and easily to be adsorbed by electrospun nanofibers membranes and other adsorbents [57,58]. Therefore, the surfaces of EFMs are partly occupied by humic acid and there are fewer places for PCP adsorption.

However, when the concentration of humic acid was higher than 10 mg L^{-1}, the removal efficiency of PCP increases with the increasing humic acid concentration. This is due to the fact that PCP can be adsorbed by humic acid molecules as well [59]. At a relative high concentration of humic acid, although PCP is hardly adsorbed by EFMs directly, it can still be adsorbed by humic acid which has been adsorbed by EFMs. Therefor the removal efficiency of PCP is in direct proportion to the concentration of humic acid.

4. Conclusion

PLGA EFMs preparing by emulsion electrospinning are polyporous and hydrophobic. The sorption kinetic data of PCP on EFMs at different solution pH indicate PCP in deprotonated form is much easier to be adsorbed, and the data are fitted better by PSOM. The sorption isotherm data in this study are fitted well by both LM and FM. The sorption capacity is about 44.69 mg g^{-1}. The hydrophobic interactions, hydrogen bonding interactions and π–π bonding interaction exist in the PCP sorption on EFMs.

HRP enzyme is successfully immobilized on EFMs. The results of degradation experiments indicate that the optimal pH for immobilized HRP is 2–4, and the removal efficiency of 83% is achieved at pH 3. However, when pH value is higher than 4.7, nearly no adsorption and degradation process occurs as the result of PCP deprotonation. The presences of humic acid can inhibit the activity of both free HRP and immobilized HRP and decrease the adsorption capacity of PCP as a result of competitive adsorption. The optimal temperature for both free HRP and immobilized HRP are 25 °C. The operational and storage stability of immobilized HRP are highly improved. Immobilized HRP shows a better stability than free HRP, which is a very attractive aspect for real application regarding a sufficiently wide range of external conditions.

Acknowledgements

This study was financially supported by the National Basic Research Program of China (973 Program, 2010CB429003), the National Science Foundation for Innovative Research Group of China (No. 51121003), and the Program of the Co-Construction with Beijing Municipal Commission of Education of China.

Appendix A. Supplementary data

Supplementary data associated with this article can be found, in the online version, at http://dx.doi.org/10.1016/j.jhazmat.2012.12.023.

References

[1] G.P. Zhang, J.A. Nicell, Treatment of aqueous pentachlorophenol by horseradish peroxidase and hydrogen peroxide, Water Res. 34 (2000) 1629–1637.
[2] W. Zheng, H. Yu, X. Wang, W. Qu, Systematic review of pentachlorophenol occurrence in the environment and in humans in China: not a negligible health risk due to the re-emergence of schistosomiasis, Environ. Int. 42 (2012) 105–116.
[3] Y. Persson, S. Lundstedt, L. Oberg, M. Tysklind, Levels of chlorinated compounds (CPs, PCPPs, PCDEs, PCDFs and PCDDs) in soils at contaminated sawmill sites in Sweden, Chemosphere 66 (2007) 234–242.
[4] W. Zheng, X. Wang, H. Yu, X. Tao, Y. Zhou, W. Qu, Global Trends, Diversity in pentachlorophenol levels in the environment and in humans: a meta-analysis, Environ. Sci. Technol. 45 (2011) 4668–4675.
[5] S.O. Agbo, E. Kuester, A. Georgi, J. Akkanen, M.T. Leppanen, J.V.K. Kukkonen, Photostability and toxicity of pentachlorophenol and phenanthrene, J. Hazard. Mater. 189 (2011) 235–240.
[6] Z. Gao, B. Du, G. Zhang, Y. Gao, Z. Li, H. Zhang, X. Duan, Adsorption of pentachlorophenol from aqueous solution on dodecylbenzenesulfonate modified nickel–titanium layered double hydroxide nanocomposites, Ind. Eng. Chem. Res. 50 (2011) 5334–5345.
[7] J.A. Zimbron, K.F. Reardon, Continuous combined Fenton's oxidation and biodegradation for the treatment of pentachlorophenol-contaminated water, Water Res. 45 (2011) 5705–5714.
[8] M. Vitkova, K. Dercova, J. Molnarova, L. Tothova, B. Polek, J. Godocikova, The effect of lignite and *Comamonas testosteroni* on pentachlorophenol biodegradation and soil ecotoxicity, Water Air Soil Pollut. 218 (2011) 145–155.
[9] R. Leyva-Ramos, L.A. Bernal-Jacome, J. Mendoza-Barron, M.M.G. Hernandez-Orta, Kinetic modeling of pentachlorophenol adsorption onto granular activated carbon, J. Taiwan Inst. Chem. Eng. 40 (2009) 622–629.
[10] Y.M. Li, Y. Zhang, J.F. Li, X.M. Zheng, Enhanced removal of pentachlorophenol by a novel composite: nanoscale zero valent iron immobilized on organobentonite, Environ. Pollut. 159 (2011) 3744–3749.
[11] R. Leyva-Ramos, P.E. Diaz-Flores, J. Leyva-Ramos, R.A. Femat-Flores, Kinetic modeling of pentachlorophenol adsorption from aqueous solution on activated carbon fibers, Carbon 45 (2007) 2280–2289.
[12] M.A. Salam, R.C. Burk, Thermodynamics, Kinetics studies of pentachlorophenol adsorption from aqueous solutions by multi-walled carbon nanotubes, Water Air Soil Pollut. 210 (2010) 101–111.
[13] W.D. Oh, P.E. Lim, C.E. Seng, A. Sujari, Bioregeneration of granular activated carbon in simultaneous adsorption and biodegradation of chlorophenols, Bioresour. Technol. 102 (2011) 9497–9502.
[14] H. Leon-Santiesteban, M. Meraz, K. Wrobel, A. Tomasini, Pentachlorophenol sorption in nylon fiber and removal by immobilized Rhizopus oryzae ENHE, J. Hazard. Mater. 190 (2011) 707–712.
[15] C. Kazunga, M.D. Aitken, A. Gold, Primary product of the horseradish peroxidase-catalyzed oxidation of pentachlorophenol, Environ. Sci. Technol. 33 (1999) 1408–1412.
[16] Y.J. Choi, H.J. Chae, E.Y. Kim, Steady-state oxidation model by horseradish peroxidase for the estimation of the non-inactivation zone in the enzymatic removal of pentachlorophenol, J. Biosci. Bioeng. 88 (1999) 368–373.
[17] E.Y. Kim, Y.J. Choi, H.J. Chae, K.H. Chu, Removal of aqueous pentachlorophenol by horseradish peroxidase in the presence of surfactants, Biotechnol. Bioprocess Eng. 11 (2006) 462–465.
[18] J.A. Zimbron, K.F. Reardon, Fenton's oxidation of pentachlorophenol, Water Res. 43 (2009) 1831–1840.
[19] J. Zhang, P. Ye, S. Chen, W. Wang, Removal of pentachlorophenol by immobilized horseradish peroxidase, Int. Biodeterior. Biodegradation 59 (2007) 307–314.

[20] H. Takahashi, B. Li, T. Sasaki, C. Miyazaki, T. Kajino, S. Inagaki, Catalytic activity in organic solvents and stability of immobilized enzymes depend on the pore size and surface characteristics of mesoporous silica, Chem. Mater. 12 (2000) 3301–3305.
[21] O. Aybastier, S. Sahin, E. Isik, C. Demir, Determination of total phenolic content in Prunella L. by horseradish peroxidase immobilized onto chitosan beads, Anal. Methods 3 (2011) 2289–2297.
[22] Y. Wang, D. Zhang, F.R. He, X.C. Chen, Immobilization of laccase by Cu^{2+} chelate affinity interaction on surface modified magnetic silica particles and its use for the removal of pentachlorophenol, Chin. Chem. Lett. 23 (2012) 197–200.
[23] M. Wissink, R. Beernink, J.S. Pieper, A.A. Poot, G. Engbers, T. Beugeling, W.G. van Aken, J. Feijen, Immobilization of heparin to EDC/NHS-crosslinked collagen, characterization and in vitro evaluation, Biomaterials 22 (2001) 151–163.
[24] E. Topoglidis, A. Cass, G. Gilardi, S. Sadeghi, N. Beaumont, J.R. Durrant, Protein adsorption on nanocrystalline TiO_2 films: an immobilization strategy for bioanalytical, Anal. Chem. 70 (1998) 5111–5113.
[25] D. Trau, R. Renneberg, Encapsulation of glucose oxidase microparticles within a nanoscale layer-by-layer film: immobilization and biosensor applications, Biosens. Bioelectron. 18 (2003) 1491–1499.
[26] C. Mateo, J.M. Palomo, G. Fernandez-Lorente, J.M. Guisan, R. Fernandez-Lafuente, Improvement of enzyme activity, stability and selectivity via immobilization techniques, Enzyme Microb. Technol. 40 (2007) 1451–1463.
[27] Y.R. Dai, J.F. Niu, J. Liu, L.F. Yin, J.J. Xu, In situ encapsulation of laccase in microfibers by emulsion electrospinning: Preparation, characterization, and application, Bioresour. Technol. 101 (2010) 8942–8947.
[28] X.L. Xu, X.L. Zhuang, X.S. Chen, X.R. Wang, L.X. Yang, X.B. Jing, Preparation of core-sheath composite nanofibers by emulsion electrospinning, Macromol. Rapid Commun. 27 (2006) 1637–1642.
[29] Y.R. Dai, L.F. Yin, J.F. Niu, Laccase-carrying electrospun fibrous membranes for adsorption and degradation of PAHs in shoal soils, Environ. Sci. Technol. (2011) 10611–10618.
[30] X. Luo, C. Xie, H. Wang, C. Liu, S. Yan, X. Li, Antitumor activities of emulsion electrospun fibers with core loading of hydroxycamptothecin via intratumoral implantation, Int. J. Pharm. 425 (2012) 19–28.
[31] L. Tian, M.P. Prabhakaran, X. Ding, D. Kai, S. Ramakrishna, Emulsion electrospun vascular endothelial growth factor encapsulated poly(L-lactic acid-co-epsilon-caprolactone) nanofibers for sustained release in cardiac tissue engineering, J. Mater. Sci. 47 (2012) 3272–3281.
[32] X.L. Xu, L.X. Yang, X.Y. Xu, X. Wang, X.S. Chen, Q.Z. Liang, J. Zeng, X.B. Jing, Ultrafine medicated fibers electrospun from W/O emulsions, J. Control. Release 108 (2005) 33–42.
[33] S.R. Bhattarai, N. Bhattarai, H.K. Yi, P.H. Hwang, D.I. Cha, H.Y. Kim, Novel biodegradable electrospun membrane: scaffold for tissue engineering, Biomaterials 25 (2004) 2595–2602.
[34] A. Greiner, J.H. Wendorff, Electrospinning, A fascinating method for the preparation of ultrathin fibres, Angew. Chem. Int. Ed. 46 (2007) 5670–5703.
[35] D. Kai, M.P. Prabhakaran, G. Jin, S. Ramakrishna, Polypyrrole-contained electrospun conductive fibrous membranes for cardiac tissue engineering, J. Biomed. Mater. Res. A 99A (2011) 376–385.
[36] J. Lin, C. Li, Y. Zhao, J. Hu, L. Zhang, Co-electrospun fibrous membranes of collagen and Zein for wound healing, ACS Appl. Mater. Interfaces 4 (2012) 1050–1057.
[37] Z. Zhong, Q. Cao, B. Jing, X. Wang, X. Li, H. Deng, Electrospun PVdF–PVC fibrous polymer electrolytes for polymer lithium-ion batteries, Mater. Sci. Eng. B-Adv. Funct. Solid-State Mater. 177 (2012) 86–91.
[38] Q.A. Feng, X. Xia, A.F. Wei, X.Q. Wang, Q.F. Wei, D.Y. Huo, A.J. Wei, Preparation of Cu(II)-chelated poly(vinyl alcohol) fibrous membranes for catalase immobilization, J. Appl. Polym. Sci. 120 (2011) 3291–3296.
[39] S. Li, Y. Fan, J. Hu, Y. Huang, W. Wu, Immobilization of *Pseudomonas cepacia* lipase onto the electrospun PAN fibrous membranes for transesterification reaction, J. Mol. Catal. B: Enzym. 73 (2011) 98–103.
[40] D.N. Tran, K.J. Balkus, Perspective of recent progress in immobilization of enzymes, Acs Catalysis 1 (2011) 956–968.
[41] X. Li, Y. Su, S. Liu, L. Tan, X. Mo, S. Ramakrishna, Encapsulation of proteins in poly(L-lactide-co-caprolactone) fibers by emulsion electrospinning, Colloids Surf. B-Biointerfaces 75 (2010) 418–424.
[42] Y.R. Dai, J.F. Niu, L.F. Yin, J.J. Xu, Y.H. Xi, Sorption of polycyclic aromatic hydrocarbons on electrospun fibrous membranes: sorption kinetics and mechanism, J. Hazard. Mater. 192 (2011) 1409–1417.
[43] P. Olivera, P. Milos, S. Dragica, S. Zeljko, R. Ksenija, K.J. Zorica, P. Radivoje, Improved covalent immobilization of horseradish peroxidase on macroporous glycidyl methacrylate-based copolymers, Appl. Biochem. Biotechnol. 5 (2012) 1288–1301.
[44] Y.P. Zhang, T.H. Liu, Q. Wang, J.H. Zhao, J. Fang, W.G. Shen, Synthesis of novel poly(N,N-diethylacrylamide-co-acrylic acid) (P(DEA-co-AA)) microgels as carrier of horseradish peroxidase immobilization for pollution treatment, Macromol. Res. 5 (2012) 484–489.
[45] H.J. Kim, Y. Suma, S.H. Lee, J.A. Kim, H.S. Kim, Immobilization of horseradish peroxidase onto clay minerals using soil organic matter for phenol removal, J. Mol. Catal. B-Enzym. 83 (2012) 8–15.
[46] H.J. Park, C.Y. Ryu, Scalable PEO–PPO–PEO triblock copolymer purification from Pluronics through competitive adsorption, Polymer 22 (2012) 5052–5059.
[47] J. Liu, J.F. Niu, L.F. Yin, F. Jiang, In situ encapsulation of laccase in nanofibers by electrospinning for development of enzyme biosensors for chlorophenol monitoring, Analyst 22 (2011) 4802–4808.
[48] D. Boyle, Effects of pH and cyclodextrins on pentachlorophenol degradation (mineralization) by white-rot fungi, J. Environ. Manage. 80 (2006) 380–386.
[49] M.G. Stapleton, D.L. Sparks, S.K. Dentel, Sorption of pentachlorphenol to Hdtma–clay as a function of ionic-strength and pH, Environ. Sci. Technol. 28 (1994) 2330–2335.
[50] F. DePaolis, J. Kukkonen, Binding of organic pollutants to humic and fulvic acids: influence of pH and the structure of humic material, Chemosphere 34 (1997) 1693–1704.
[51] Q. Yu, R. Zhang, S. Deng, J. Huang, G. Yu, Sorption of perfluorooctane sulfonate and perfluorooctanoate on activated carbons and resin: kinetic and isotherm study, Water Res. 43 (2009) 1150–1158.
[52] W.H. Cheung, Y.S. Szeto, G. McKay, Intraparticle diffusion processes during acid dye adsorption onto chitosan, Bioresour. Technol. 98 (2007) 2897–2904.
[53] M. Yuan, S. Tong, S. Zhao, C.Q. Jia, Adsorption of polycyclic aromatic hydrocarbons from water using petroleum coke-derived porous carbon, J. Hazard. Mater. 181 (2010) 1115–1120.
[54] Y.C. Hseu, W.C. Chang, H.L. Yang, Inhibition of human plasmin activity using humic acids with arsenic, Sci. Total Environ. 273 (2001) 93–99.
[55] D. Sutlovic, M.D. Gojanovic, S. Andelinovic, D. Gugic, D. Primorac, Taq polymerase reverses inhibition of quantitative real time polymerase chain reaction by humic acid, Croat. Med. J. 46 (2005) 556–562.
[56] G.Y. Kim, X.F. Wang, H. Ahn, A. Son, Gene quantification by the nano gene assay is resistant to inhibition by humic acids, Environ. Sci. Technol. 45 (2011) 8873–8880.
[57] N. Kawasaki, F. Ogata, I. Yamaguchi, A. Fujii, Removal of orange II, methylene blue and humic acid by ozone-activated carbon combination (OZAC) treatment, J. Oleo Sci. 57 (2008) 391–396.
[58] V. Thavasi, G. Singh, S. Ramakrishna, Electrospun nanofibers in energy and environmental applications, Energy Environ. Sci. 1 (2008) 205–221.
[59] O. Bouras, J. Bollinger, M. Baudu, Effect of humic acids on pentachlorophenol sorption to cetyltrimethylammonium-modified, Fe- and Al-pillared montmorillonites, Appl. Clay Sci. 50 (2010) 58–63.